Artifacts in FDG PET and PET/CT

9

Masashi Kawaguchi, Ukihide Tateishi,
Tomio Inoue, and E. Edmund Kim

As the number of clinical positron emission tomography (PET) units is increasing, interpretation of PET images requires knowledge of the possible pitfalls that may occur because of artifacts and mimic pathology. In addition, the advent of combined PET/computed tomography (CT) scanners in clinical imaging practice has brought its own specific pitfalls and artifacts. These artifacts may be caused by various factors such as injection, attenuation material, image reconstruction, contamination, patient movements, and pathologic variants. Knowledge of the normal distribution of fluorodeoxyglucose (FDG) and its pathologic variation is essential before interpreting PET scans as well as an awareness of potential false positive and negative cases that can occur. With attention to detail in the preparation of patients, together with appropriate imaging protocols and experience in interpretation, many pitfalls can be avoided.

M. Kawaguchi • U. Tateishi, M.D., Ph.D. (✉)
T. Inoue, M.D., Ph.D.
Department of Radiology, Yokohama City University Graduate School of Medicine,
Yokohama 236-0004, Japan
e-mail: utateish@yokohama-cu.ac.jp; tomioi@yokohama-cu.ac.jp

E.E. Kim, M.D., M.S.
Departments of Nuclear Medicine and Diagnostic Radiology, The University of Texas MD Anderson Cancer Center and Medical School,
Houston, TX 77030, USA

Graduate School of Convergence Science and Technology, Seoul National University,
Seoul, South Korea
e-mail: ekim@mdanderson.org

Normal Whole-Body FDG Distribution

On whole-body PET performed between 1 and 2 h following intravenous administration of FDG, the brain, heart, and urinary tract are the most prominent sites of tracer accumulation (Fig. 9.1).

In the brain, there is high uptake in the cortex and basal ganglia irrespective of different substrates as glucose is the predominate substrate for brain metabolism. The liver and spleen are associated with slightly higher FDG activity than blood pool levels and are reliably identified in the abdomen, as are the kidneys. Some lymphoid tissue is normally quite active, including the tissues of Waldeyer's ring where the tonsils can show moderate uptake, and that is usually symmetrical. Salivary glands also show low to moderate symmetrical uptake. Thymic activity is commonly seen in children and can also be seen in adolescents and young adults after chemotherapy as a result of thymic rebound phenomenon [1]. Cardiac activity is variable and depends to some extent on substrate availability such as fatty acids and glucose. Glandular tissue of the breast is associated with low-level uptake in younger woman. Bone marrow is normally associated with modest FDG uptake, roughly equivalent to liver. The bowel is seen to varying degrees, as is the stomach because of widely variable levels of

E.E. Kim et al. (eds.), *Clinical PET and PET/CT: Principles and Applications*,
DOI 10.1007/978-1-4419-0802-5_9, © Springer Science+Business Media New York 2013

Fig. 9.1 48-y-old, female. Normal distribution of FDG 1 h following intravenous tracer administration. Attenuation-corrected anterior maximum intensity projection (MIP) image. Intense tracer activity in the brain and bladder. In the neck, palatine tonsil lymphoid tissue tracer activity (*small arrow*) is seen. Inferior to the heart is low-level gastric tracer activity (*arrowhead*) and the outlines of the liver, spleen, and kidneys are discernable. In premenopausal women cyclical right ovarian uptake of FDG is seen in pelvis (*large arrow*)

Fig. 9.2 Brown adipose tissue (BAT) FDG uptake. Anterior MIP image of 9-y-old boy. Intense FDG activity is present symmetrically at the base of neck, upper mediastinum, supraclavicular regions, axillae, paravertebral locations at the thoracic spine

FDG uptake in the alimentary tract. Marrow is commonly identified in the vertebral bodies, pelvis, hips, proximal long bones, and the sternum. The level of FDG uptake in children is higher in bone marrows than in adults. Uptake of FDG into active, non-rested muscle is a potential cause of misinterpretation of FDG PET scans although with combined PET/CT, this is less likely. Activities such as talking can lead to muscle uptake in the neck and larynx. Asymmetric uptake can be seen in laryngeal muscles in patients with vocal code palsies [2]. In premenopausal women, FDG uptake of cyclical ovarian and uterine has been described [3]. Activity of uterine cavity is seen at mid cycle and during menses and ovarian activity can be seen at mid cycle.

Brown adipose tissue (BAT) expresses a unique mitochondrial uncoupling protein that permits direct heat generation from fatty acid oxidation in response to cold exposure, ingestion of food, or increased sympathetic activity. This process requires an increased supply of adenosine triphosphate (ATP), which in turn is provided by an increase in glycolytic metabolism. It is recognized that intense increased FDG activity can localize to adipose tissue in the neck, supraclavicular regions, axillae, paravertebral locations at the thoracic spine, mediastinum, and occasionally subdiaphragmatic and perinephric fat (Fig. 9.2). This phenomenon is seen more often in young patients, females, and slender patients [4].

Artifacts in FDG PET and PET/CT

Injection-related artifacts may interfere with image interpretation (Fig. 9.3). A partly infiltrated injection causes a reconstruction artifact across the trunk. It also results in inaccuracy of the standard uptake value (SUV). If the injection leak on FDG PET images is demonstrated, the SUV derived from these images should be carefully evaluated. Following the subcutaneous extravasations of FDG solution, the tracer may flow into the lymphatic channel and may be trapped in local lymph nodes [5]. It mimics an abnormal FDG uptake in the lymph node metastases. The tracer should be administered on the opposite site to the known lesion. Increased levels of insulin in the peri-injection period cause extracardiac uptake in diabetic patients or patients who did not fast [6].

On PET/CT scanners, the emission data can be corrected for photon attenuation using the CT scan to generate an attenuation map. Doing so confers the following advantages: there is less statistical noise from the CT compared with germanium 68 (^{68}Ge) transmission data on stand-alone PET scanners; the scanning time for CT is much shorter then for radionuclide imaging, thus reducing overall scanning time by 15–20 min; and the need for PET transmission hardware and the cost of replacing germanium source rods are eliminated [7].

There is a potential risk of overestimating the true FDG activity with CT-based attenuation correction. When the CT images are used to perform attenuation correction of the PET projection data, dense objects can cause apparent hot spot artifacts on the PET, as well as beam hardening artifact on CT images. Metallic prosthetic implants and high-density medical devices such as dental fillings, hip prosthetics, surgical clips, metallic stents, drainage tubes, or chemotherapy ports cause high CT numbers and generate streaking artifacts on CT images because of their high photon absorption [8,9]. This increase in CT numbers results in high PET attenuation coefficients, which lead to an overestimation of the PET activity in that lesion and thereby to false-positive PET imaging (Figs. 9.4, 9.5, 9.6, and 9.7).

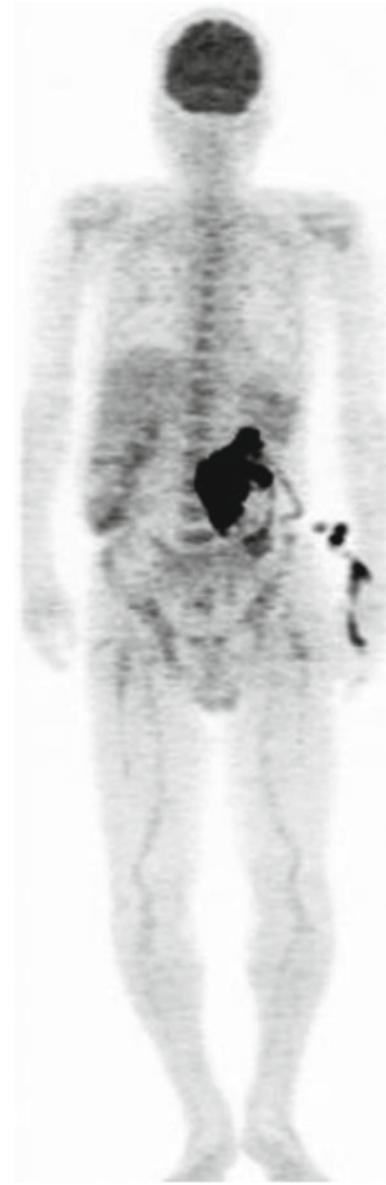

Fig. 9.3 Anterior MIP image of a patient with retroperitoneal tumor (*small arrow*). Note increased uptake in nephrostomy tube (*large arrow*). Subcutaneous extravasation and superficial contamination of FDG solution are seen in left forearm (*arrowhead*)

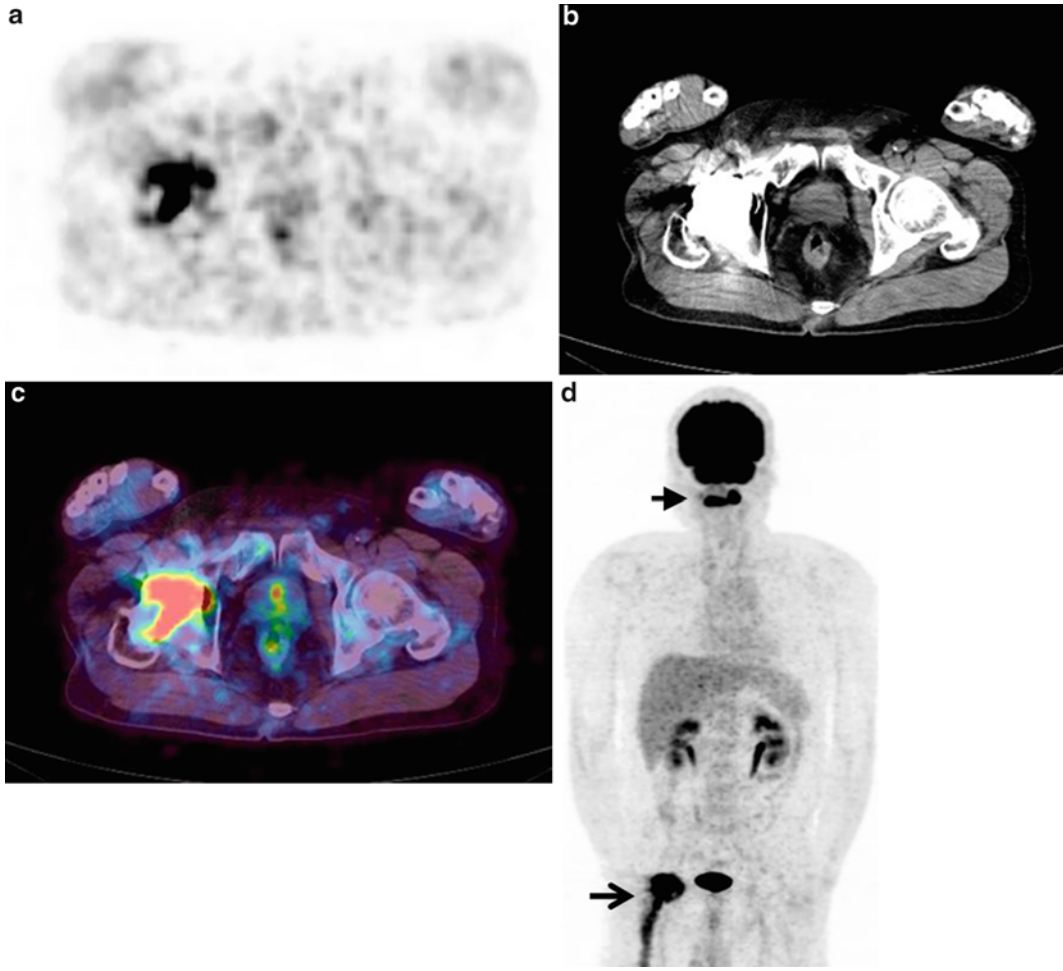

Fig. 9.4 Artifacts because of metallic dental fillings (*arrowhead*) and hip prosthetics (*arrows*). PET scan shows apparent increased activity in oral cavity and right hip joint

Intravenous or oral agents such as iodine and barium sulfate are administered to improve the quality of CT images by delineating vessels and soft tissues [10]. High contrast concentration results in high CT numbers and streaking artifacts on CT images. Therefore, contrast media also can cause an overestimation of tracer uptake and produce false-positive PET results similar to metallic implants (Fig. 9.8).

Such artifacts can be recognized by review of the non-attenuation-corrected filtered back projection PET images (Fig. 9.9). It is important to verify attenuation-corrected images against non-attenuation corrected images to avoid false-positive results. Regarding the image reconstruction, attenuation correction is essentially needed to obtain the quantitative image data such as the SUV.

Present statistical image reconstruction algorithms can yield focal apparent increased activity from movement artifacts or generalized noise. Transaxial attenuation-corrected images generated using ordered-subset expectation maximization reconstruction method with three interactions and eight subsets show multiple tiny apparent foci of increased FDG activity in the liver of a large patient. It is advisable to have non-attenua-

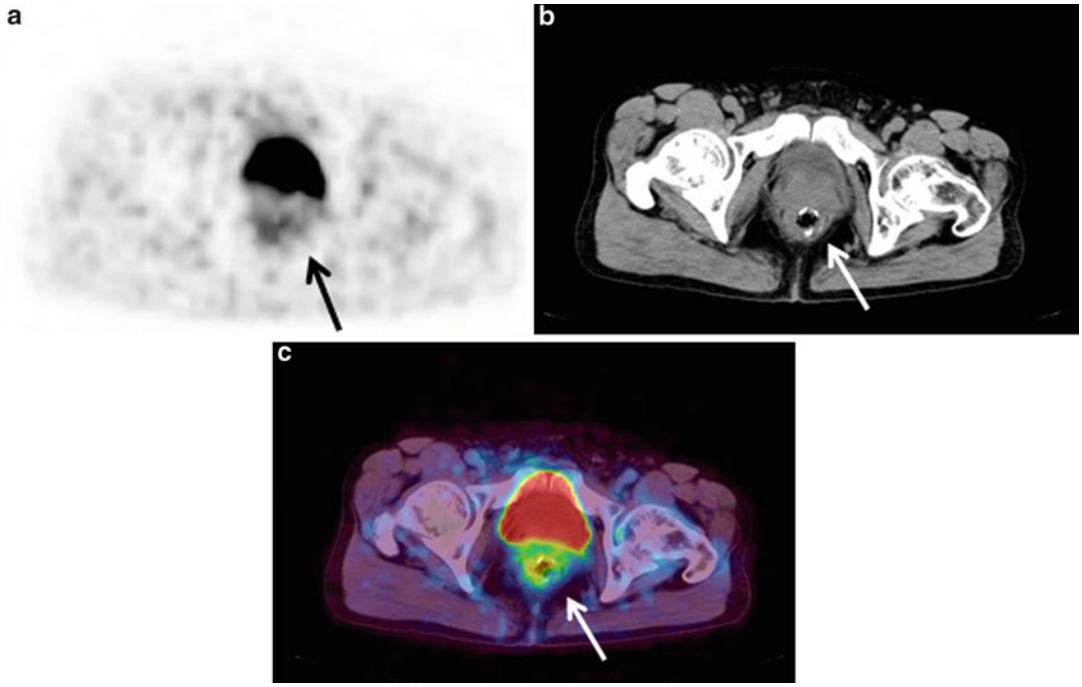

Fig. 9.5 55-y-old man who underwent resection for rectal cancer. Transaxial PET image through pelvis reveals focus of increased tracer uptake in rectum (*arrow*), suggestive of local recurrence. Corresponding CT scan shows surgical clip in place (*white arrow*)

tion-corrected filtered back projection images for confirmation of such suspect abnormalities.

Urinary contamination is sometimes observed on FDG PET images. Because urinary contamination is usually superficial activity on the skin or clothes, it is easily recognized as artifact.

Patient movements degrade the image quality of FDG PET. Whole-body FDG PET imaging can lead to an unusual appearance if the patient moves between the bed scan positions, with the upper part of an arm, for example, being visible in the higher scanning positions but absent or "amputated" lower down when moved out of the field of view for lower scanning positions (Fig. 9.10).

Respiratory motion during scanning causes artifact in PET/CT imaging. The artifact is caused by the discrepancy between the chest position on the CT image and the chest position on the PET image. Each bed position of the PET scan may take 2–5 min to acquire during free breathing and resulting in images representing an average position of respiratory cycle. This may lead to misregistration of lung nodules by 15 mm [11]. Difference between the PET and CT acquisitions may be maximal at the level of the diaphragm which may lead to artifacts, the most common being an apparent area of reduced activity at the diaphragmatic surface when the CT data are used for attenuation correction. Additionally, this can lead to apparent mispositioning of liver metastases into the lung base (Figs. 9.11 and 9.12).

Motion artifacts lead to two major effects: First, it affects the accuracy of quantification, producing a reduction of the measured SUV. Second, the apparent lesion volume is overestimated. Respiratory gating by applying a multiple-frame capture technique, with which PET data are

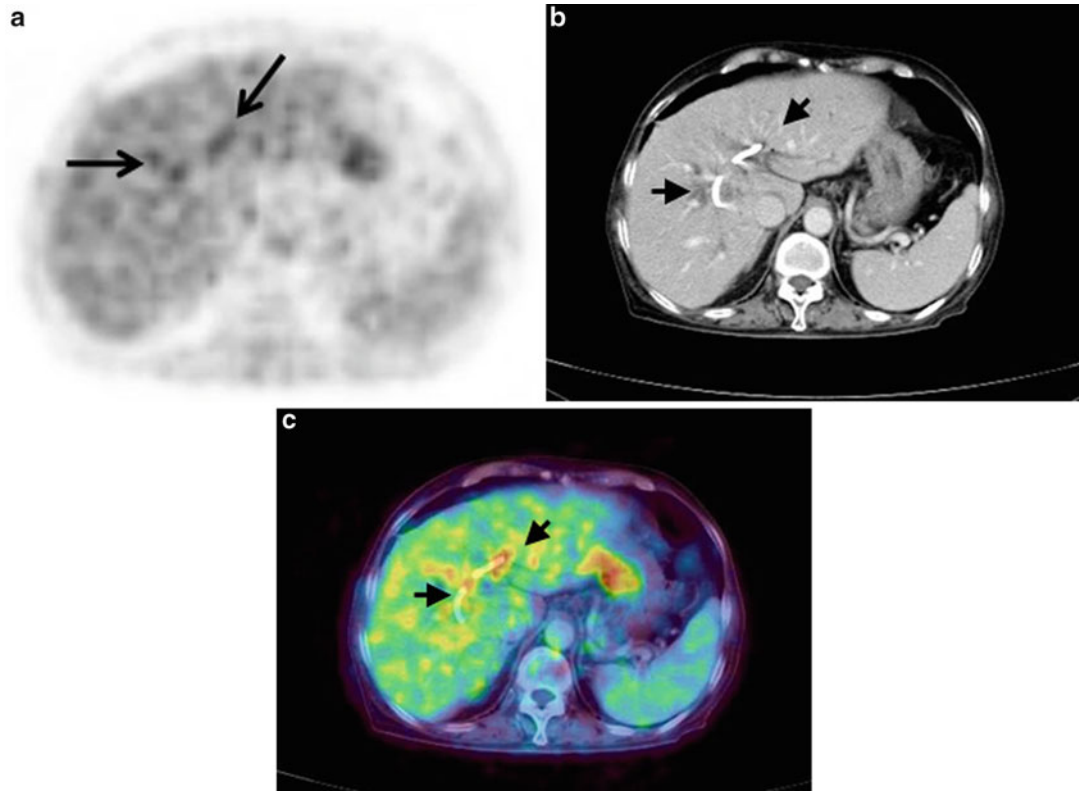

Fig. 9.6 73-y-old woman with extrahepatic bile duct cancer. Transaxial PET image reveals focus of increased tracer uptake in liver (*arrows*), suggestive of tumor invasion. Corresponding CT scan shows bile duct tube in place (*arrowheads*)

acquired in synchronization with the respiratory motion, compensates for these effects.

A number of benign diseases may cause significant uptake of FDG that may simulate malignant lesion. In the chest, active tuberculosis, sarcoidosis, and histoplasmosis have been reported as showing increased FDG uptake (Fig. 9.13) [12]. These disorders may lead to FDG uptake (SUV) in the borderline or low-malignant range. Inflammation in any tissue may cause increased FDG uptake. Common sites of inflammatory activity are surgical or radiotherapeutic areas (Fig. 9.14), and the activities may last for several weeks after therapy.

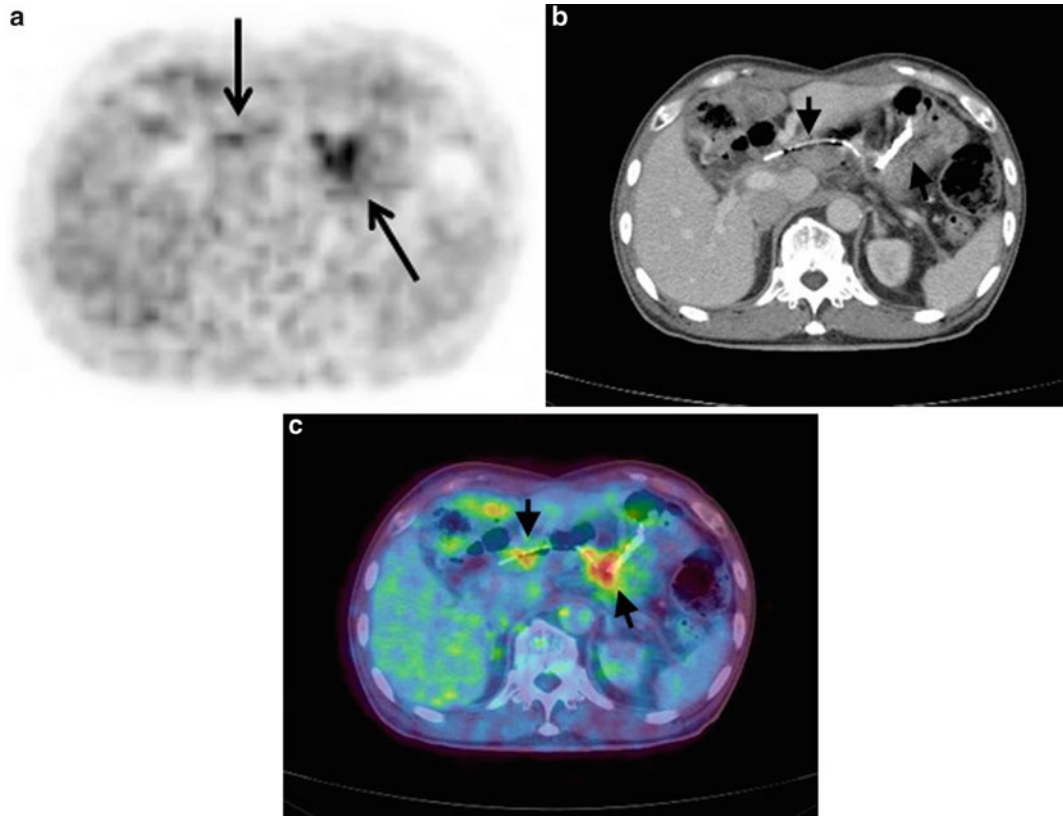

Fig. 9.7 76-y-old man after gastorectomy and pancreatoduodenectomy for gastric cancer and pancreatic cancer. Transaxial PET image reveals focus of increased tracer uptake in residual stomach and pancreas (*arrows*), suggestive of recurrence. Corresponding CT scan shows surgical clip in the stomach and pancreatic duct tube (*white arrow*)

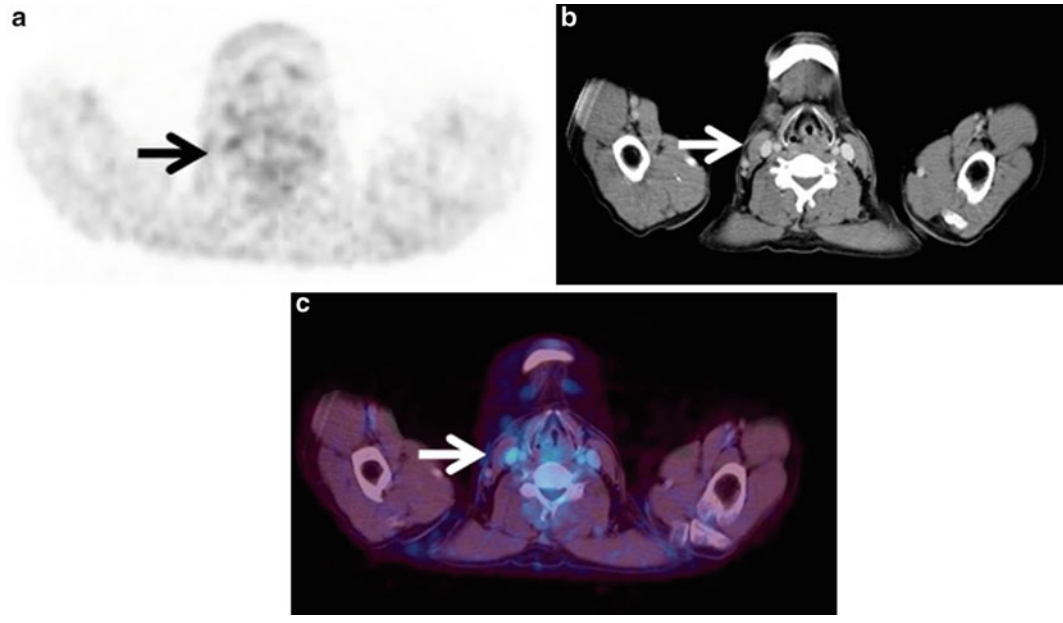

Fig. 9.8 Focal nodal uptake is seen in the right neck on FDG PET (*arrow*). It apparently seems to be lymph node metastasis although CT scan shows intravenous contrast medium in right common carotid artery and internal jugular vein (*white arrow*) at the site

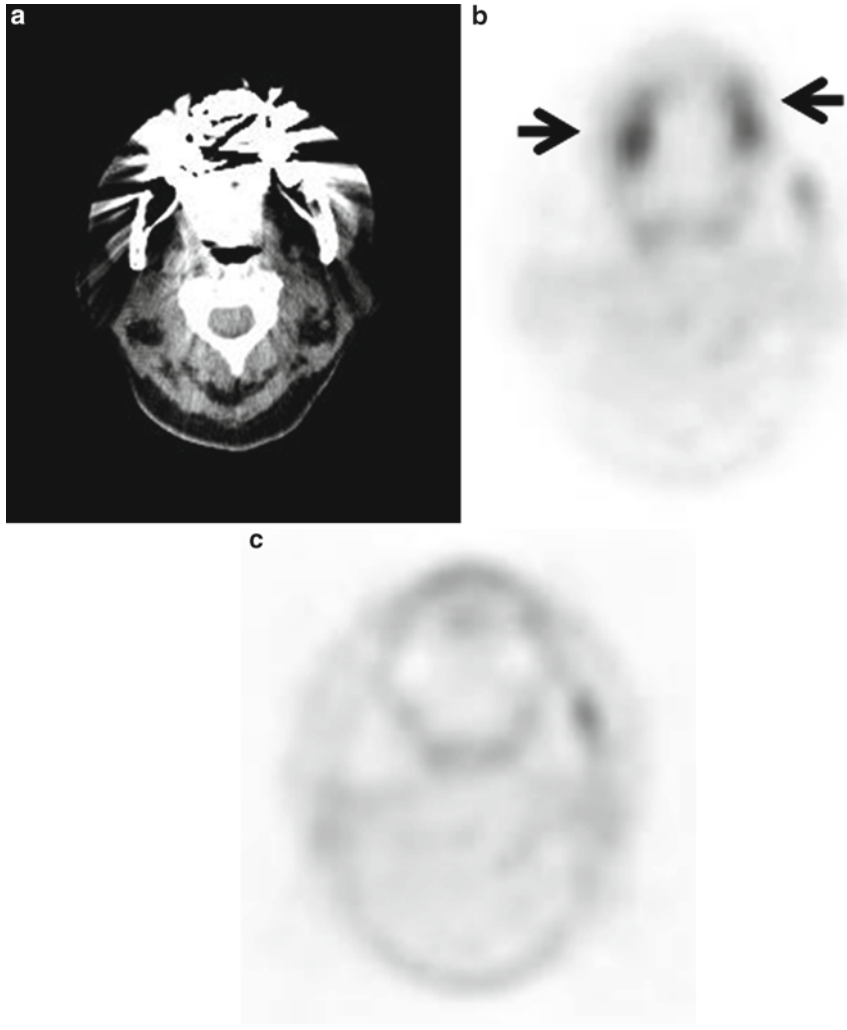

Fig. 9.9 High-density metallic implants generate streaking artifacts and high CT numbers on CT image. High CT numbers will then to be mapped to high PET attenuation coefficients, leading to overestimation of activity concentration (*arrows*). PET images without attenuation correction help to rule out metal induced artifacts

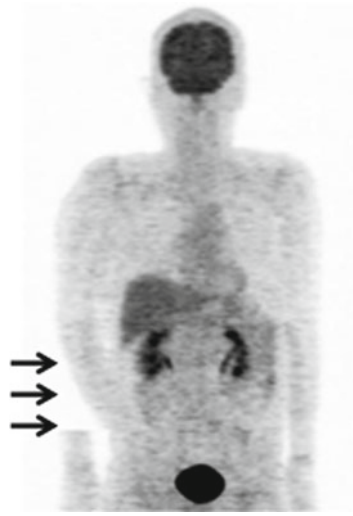

Fig. 9.10 FDG PET MIP image shows an unusual appearance with discontinuous activity in the right forearm (*arrows*) as a result of patient's movements between bed scan positions

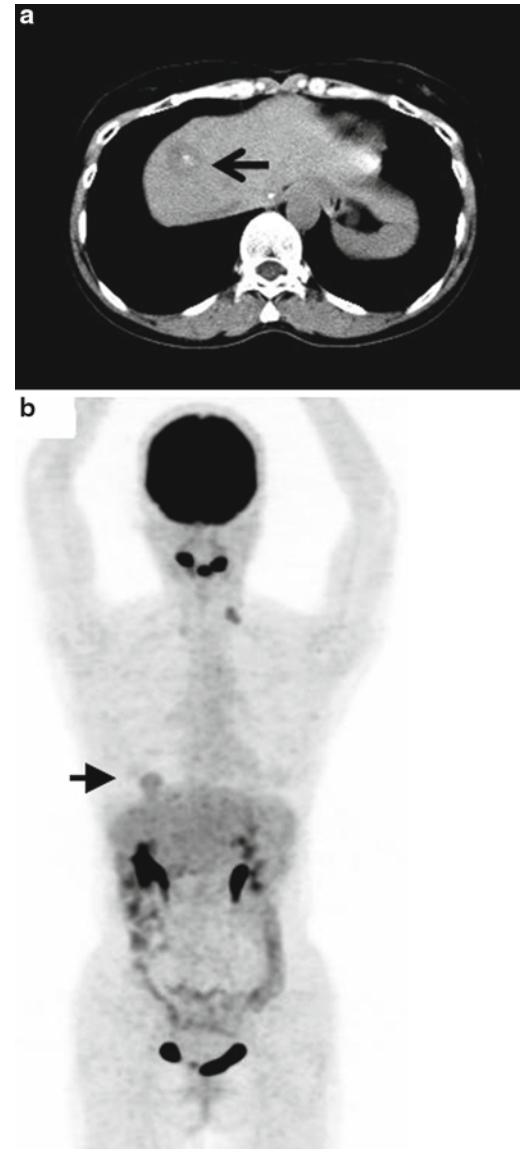

Fig. 9.11 55-y-old woman with liver metastasis of colon cancer. Lesion at dome of liver (*arrow*) is mislocalized to right lung base (*arrowhead*) because of respiratory mismatch on PET images with CT attenuation correction

Fig. 9.12 46-y-old woman with peritoneal dissemination of ovary cancer. Lesion at dome of liver (*arrow*) is mislocalized to right lung (*arrowhead*) because of respiratory motion

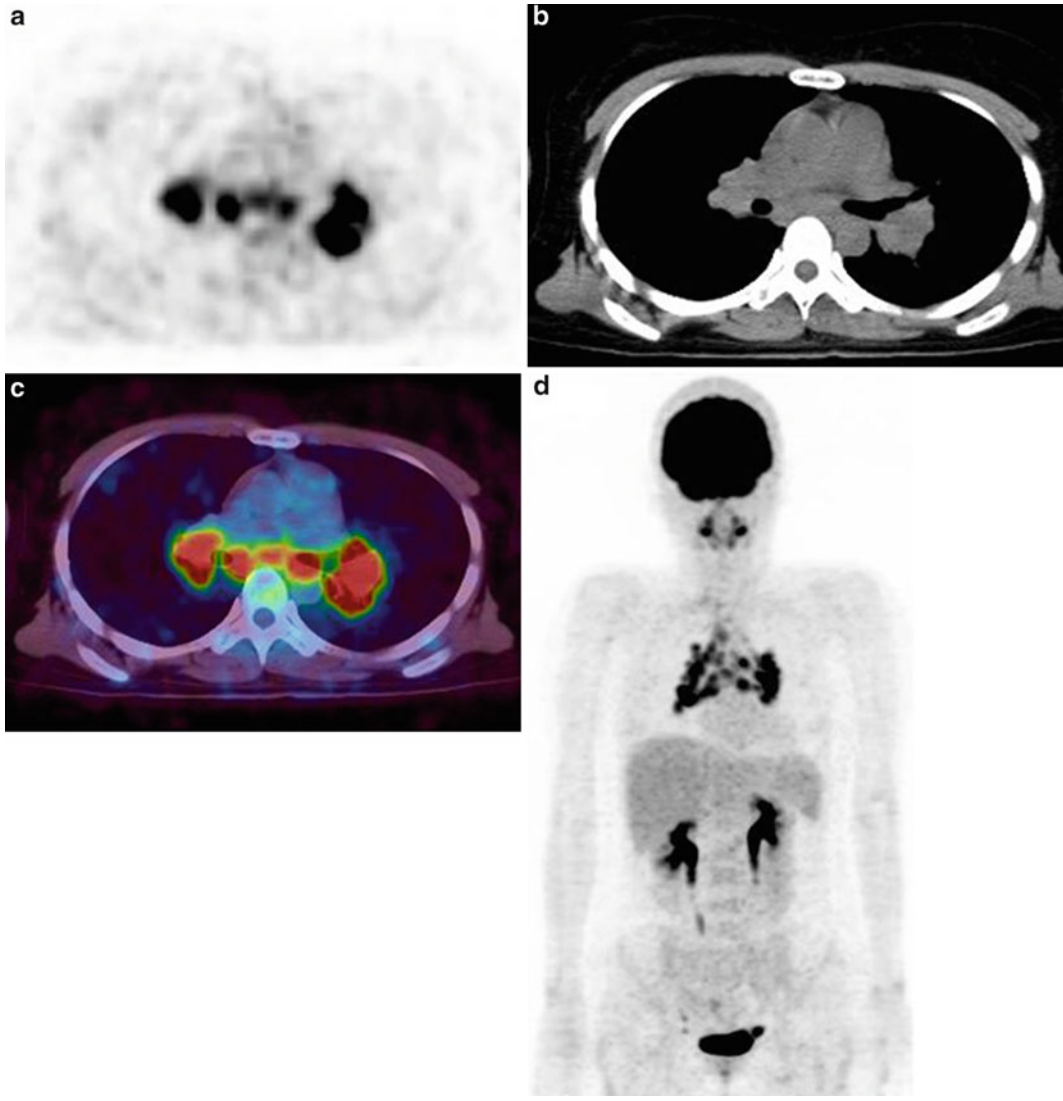

Fig. 9.13 Patterns of FDG PET in sarcoidosis. Increased FDG uptake involving enlarged lymph nodes in the bilateral mediastinum and pulmonary hila

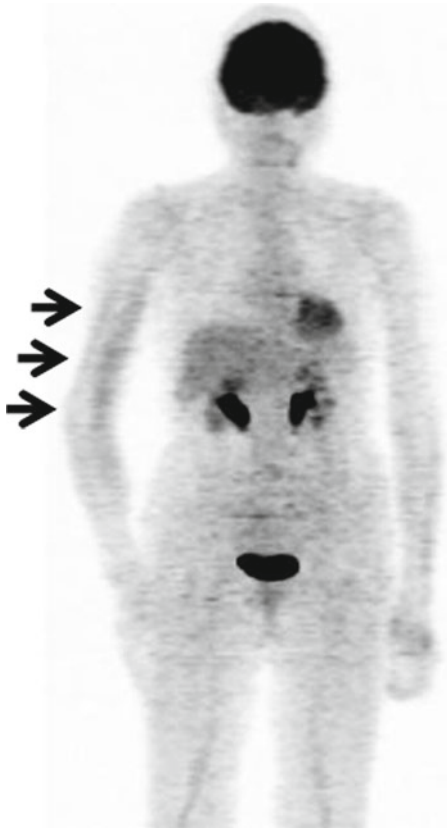

Fig. 9.14 Patient with previous radiotherapy to the right arm for malignant fibrous histiocytoma. MIP image of FDG PET shows increased uptake at the right arm (*arrows*). This abnormal uptake is a result of postradiotherapy inflammation

References

1. Kawano T, Suzuki A, Ishida A, Takahashi N, Lee J, Tayama Y, et al. The clinical relevance of thymic fluorodeoxyglucose uptake in pediatric patients after chemotherapy. Eur J Nucl Med Mol Imaging. 2004;31:831–6.
2. Kamel EM, Goerres GW, Burger C, von Schulthess GK, Stenert HC. Recurrent laryngeal nerve palsy in patients with lung cancer: detection with PET-CT image fusion: report of six cases. Radiology. 2002;224:153–6.
3. Lerman H, Mtese U, Grisaru D, Fishman A, Lievshitz G, Even-Sapir E. Normal and abnormal ^{18}F-FDG endometrial and ovarian uptake in pre- and postmenopausal patients: assessment by PET/CT. J Nucl Med. 2004;45:266–71.
4. Yeung HWD, Grewal RK, Gonen M, et al. Patterns of ^{18}F-FDG uptake in adipose tissue and muscle: a potential source of false-positives for PET. J Nucl Med. 2003;44:1789–96.
5. Alibazoglu H, Megremis D, Ali A, et al. Injection artifact on FDG-PET imaging. Clin Nucl Med. 1998;23:264–5.
6. Minn H, Nuutila P, Lindholm P, et al. In vivo effects of insulin on tumor and skeletal muscle glucose metabolism in patients with lymphoma. Cancer. 1994;73:1490–8.
7. Nakamoto Y, Osman M, Cohade C, et al. PETCT: comparison of quantitative tracer uptake between germanium and CT transmission attenuation-corrected scans. J Nucl Med. 2002;43(9):1137–43.
8. Goerres GW, Hany TF, Kamel E, et al. Head and neck imaging with PET and PET/CT: artefacts from dental metallic implants. Eur J Nucl Med. 2002;29:369–70.
9. Kamel EM, Burger C, Buck A, von Schulthess GK, Goerres GW. Impact of metallic dental implants on CT-based attenuation correction in a combined PET/CT scanner. Eur Radiol. 2003;13:724–8.
10. Antoch G, Freudenberg LS, Egelhof T, et al. Focal tracer uptake: a potential artifact in contrast-enhanced dual-modality PET/CT scans. J Nucl Med. 2002;43:1339–42.
11. Goerres GW, Kamel E, Seifert B, Burger C, Buck A, Hany TF, et al. Accuracy of image coresistration of pulmonary lesions in patients with non-small cell lung cancer using an integrated PET/CT system. J Nucl Med. 2002;43:1469–75.
12. Cook GJR, Fogelman I, Maisey MN. Normal physiological and benign pathological variants of F-18 deoxyglucose PET: potential for error in interpretation. Semin Nucl Med. 1996;26:308–24.